JOURNAL OF MATERIALS SCIENCE 15 (1980) 2701–2708

Effect of high pressure on the crystallization of an amorphous $Fe_{83}B_{17}$ alloy

WEN-KUI WANG*, HIROSHI IWASAKI, KAZUAKI FUKAMICHI
The Research Institute for Iron, Steel and Other Metals, Tohoku University, Sendai 980, Japan

Amorphous Fe–17 at %B alloy prepared by a splat-quenching technique was annealed at temperatures ranging from 250 to 500° C for different periods. A time–temperature transformation diagram has been constructed from X-ray diffraction examination of annealed samples. On annealing the alloy at a pressure of 50 kbar†, an appreciable retardation of crystallization was observed. The crystalline phase precipitated first from the amorphous matrix at 1 bar. This was α-Fe containing a small amount of boron, but at 50 kbar this was a mixture of α-Fe(B) and intermetallic phase Fe_3B. Under the increased pressure of 100 kbar the mode of the crystallization was further changed and Fe_3B became the first precipitating phase. Preferential formation of Fe_3B under pressure can be explained assuming a modified dense-random packing model for the amorphous structure.

1. Introduction

A number of metal–metalloid systems are known to be prepared in the amorphous form by splat-quenching. The amorphous state in these materials is substantially metastable and transformation into the crystalline state takes place on annealing. During this process various kinds of transient crystalline phases appear depending on temperature and period of annealing. A stable crystalline state, which in most cases is a mixture of two phases, is reached after prolonged annealing at relatively high temperatures [1]. Structural characteristics of the transformation can be expressed well in a time–temperature transformation (T–T–T) diagram and Masumoto and his co-workers [2–4] established the diagram for several binary and ternary alloys.

When amorphous alloys are subjected to high pressure, interatomic distances are decreased and space available for atomic movement is contracted. Hence some change is expected to be introduced into their crystallization behaviour. For $Pd_{75}Ag_5Si_{20}$ [5] the temperature of onset of crystallization was shown to shift appreciably towards higher temperatures. In addition to the pressure induced retardation of crystallization, formation of a metastable phase with a crystal structure entirely different from that appearing at atmospheric pressure was observed for $Pd_{80}Si_{20}$ [6]. These studies showed that pressure may possibly alter the mode of transformation of amorphous alloys greatly.

The iron–boron alloy is one of the metallic glasses which have received much attention recently owing to its interesting physical properties [7–9]. Using X-ray and electron diffraction as well as Mössbauer spectroscopy techniques, structural studies were made on the alloy. Crystalline phases that appeared successively on annealing were identified and the observed change in the physical properties was associated with the structural sequence [10–12]. According to the results of these studies the crystallization starts by precipitation of α-Fe and, subsequently or simultaneously depending on the alloy composition, metastable phases such as $Fe_{23}B_6$, $Fe_{3.5}B$ and

*On leave from Institute of Physics, Academia Sinica, Beijing, China.
†1 kbar = 0.1 GPa.

0022–2461/80/112701–08$02.80/0

Fe_3B appear. In the alloys containing boron less than 17 at%, precipitation of α-Fe always occurs first, while in the boron-rich alloys simultaneous precipitation of α-Fe and one of the metastable phases occurs. The most stable state of the alloy is a mixture of α-Fe and Fe_2B.

The purpose of the present work is to investigate experimentally how the application of pressure affects the crystallization behaviour of the amorphous iron–boron alloy. The alloy with a boron content of 17 at% has been chosen, which corresponds to the eutectic composition as well as the critical composition across which the crystallization sequence changes and the composition seemingly most susceptible to external effects. Though many investigations were made previously, no T–T–T diagram of the alloy was constructed. Before doing high-pressure experiments in the present work, structural studies were made on the alloy annealed at various temperatures for different periods of time. The results have been summarized in the T–T–T diagram at atmospheric pressure, which proves to be indispensable in recognizing the effects of pressure.

2. Experimental procedures

The amorphous alloy samples were prepared by rapid quenching from the melt using the roller-type quenching apparatus [13]. The velocity of revolution of the rollers of 200 mm diameter, was in the range of 3000–6000 rpm. The samples were in the form of a thin strip 1 mm wide and 50 μm thick. The composition was determined by chemical analysis.

The methods of high-pressure experiments and X-ray examination of the pressure-annealed samples were identical to those in our previous works [6, 14] and are not described here. The only difference was in the use of Fe$K\alpha$ radiation instead of Cu$K\alpha$ radiation for phase identification. High purity (99.999%) iron, obtained by electron beam floating-zone melting [15], was used as a standard material for the lattice constant determination.

3. Experimental results

3.1. T–T–T diagram of $Fe_{83}B_{17}$ alloy

Fig. 1 shows the T–T–T diagram constructed for the alloy. Filled, half-filled and open circles represent the structures found in the alloy annealed under various conditions. The diagram demonstrates that crystallization proceeds in two steps with increasing time or temperature: first α-Fe precipitates and then the depleted amorphous matrix changes into Fe_3B. Although the small-grained precipitates give only broadened diffraction lines, comparison of their X-ray pattern with that of a high-purity iron clearly shows that the α-Fe has a slightly expanded lattice ($a = 2.867$ Å)* compared with pure α-Fe ($a = 2.866$ Å), indicating that it has dissolved a small amount of boron. Since the generally accepted atomic size of boron is smaller than that of iron, the boron atoms are thought to be

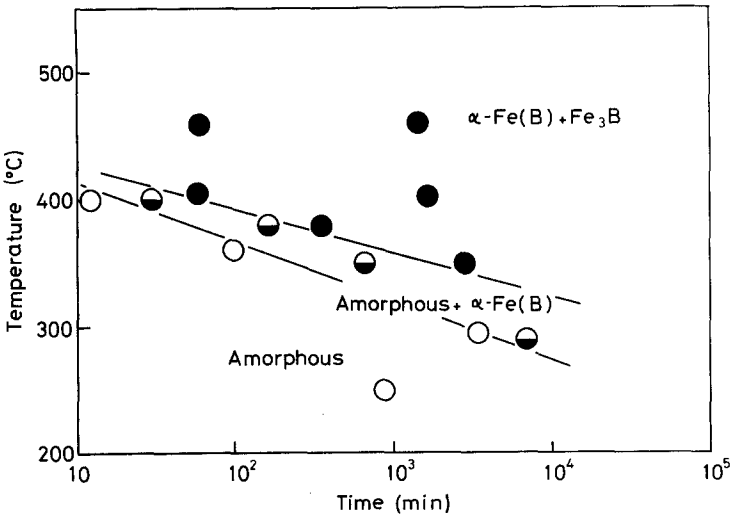

Figure 1 Time-temperature transformation diagram of amorphous $Fe_{83}B_{17}$ alloy on annealing at 1 bar.

*1 Å = 0.1 nm.

included in the iron lattice not substitutionally but interstitially. Hereafter, the precipitating phase is designated as α-Fe(B). Fe_3B is a metastable phase having the Ni_3P type structure†. The lattice constants of this tetragonal phase have been measured to be $a = 8.65_0$ Å and $c = 4.28_7$ Å, in agreement with those given by Walter *et al.* [11]. In Fig. 1 it is noted that crystallization occurs at 350° C when the alloy is kept for a period longer than 10^3 min, the temperature being considerably lower than the crystallization temperature T_c previously reported. In many investigations [8, 12, 16] T_c was determined on continuous heating and was therefore dependent on the rate at which the temperature was raised. In addition, the mode of transformation, i.e. two steps or a single step, seems to be dependent on the heating rate. In Fig. 1 the region which represents the state of the alloy α-Fe(B) plus amorphous matrix becomes narrow on moving to the left. If calorimetric measurement is performed on continuous heating at a rate as high as 20 K min^{-1}, as it was in [16], a single peak indicative of a single step transformation may be observed owing to a lack of resolution. It is therefore not legitimate to determine the mode of transformation on the basis of measurements in which the sample temperature is rapidly changed.

3.2. Crystallization under a pressure of 50 kbar

Fig. 2a shows an X-ray diffraction pattern of the alloy annealed at 50 kbar and 405° C for 600 min. Only a diffuse halo is observed, indicating that the alloy remains in the amorphous state. On the other hand annealing at 1 bar and the same temperature only for 60 min changes the alloy into the crystalline state (Fig. 1). At 50 kbar even after annealing at 340° C for as long as 38×10^3 min, part of the alloy is still amorphous, giving the X-ray diffraction pattern shown in Fig. 2b. Several diffraction lines with weak intensities are seen superimposed on the halo pattern and can be indexed as the lines from α-Fe(B) and Fe_3B. Completion of the crystallization is observed after annealing at a higher temperature of 460° C for 180 min as shown in Fig. 2c. The measured lattice constant of α-Fe(B) is 2.868 Å, which shows that it contains more boron as interstitial atoms than the α-Fe precipitating at 1 bar. Those of Fe_3B are $a = 8.64_7$ Å and $c = 4.28_2$ Å. Table I lists the observed and calculated *d*-values as well as intensities of the reflection of Fe_3B formed at 50 kbar. The atomic positional parameters used in the calculation are those of the Ni_3P type structure [17]. Agreement between the observed and calculated values is generally good, indicating that there is no significant

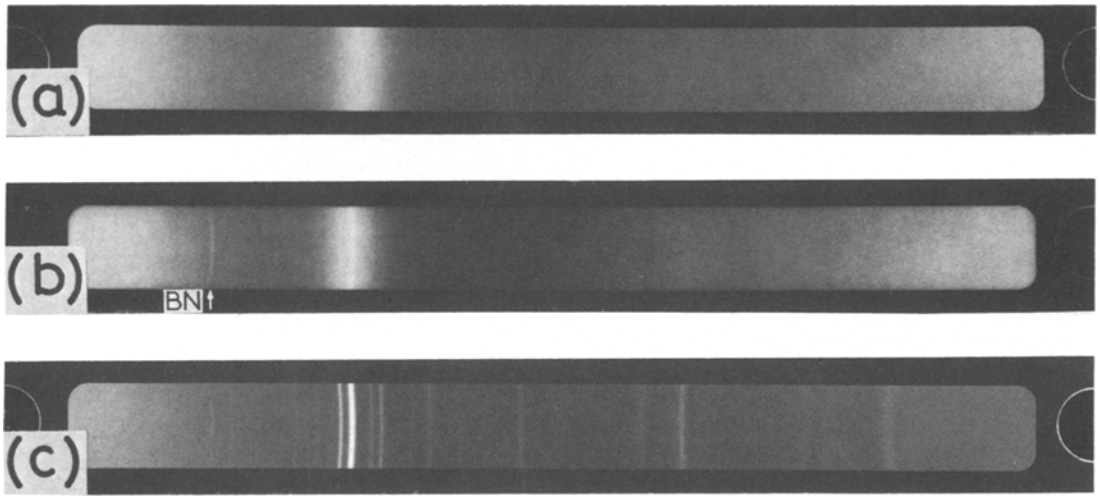

Figure 2 X-ray diffraction patterns of amorphous $Fe_{83}B_{17}$ alloy annealed (a) at 50 kbar and 405° C for 600 min, (b) at 50 kbar and 340° C for 38 × 10^3 min and (c) at 50 kbar and 460° C for 180 min.

†Herold and Köster [10] designated this phase as $Fe_{3.5}B$, but in the present paper we adopt the normal nomenclature Fe_3B based on the structural similarity.

TABLE I X-Ray diffraction data for Fe_3B formed at 50 kbar. FeKα radiation, Ni_3P type structure BCT cell: $a = 8.64_7$ Å, $c = 4.28_2$ Å, $I = m \cdot |F(h\,k\,l)|^2 \cdot L_p$

$h\,k\,l$	d (Å)		I/I_o	
	observed	calc.	observed	calc.
1 1 0	–	6.114	–	3
2 0 0	–	4.324	–	< 1
1 0 1	–	3.837	–	6
2 2 0	3.05_9	3.057	W	5
2 1 1	2.87_2	2.870	VW	1
3 1 0	2.73_4	2.734	W	7
3 0 1	2.39_0	2.391	M	26
4 0 0	2.15_2	2.162	W	4
0 0 2		2.141		5
3 2 1	2.08_8	2.092	S	100
3 3 0	2.02_7*	2.038	VS	18
1 1 2		2.021		41
4 2 0	1.92_6	1.934	M	48
2 0 2		1.919		9
4 1 1	1.87_9	1.883	M	25
2 2 2	1.75_6	1.754	W	11
5 1 0	1.69_0	1.696	M	1
3 1 2		1.686		32
5 0 1	–	1.604	–	2
4 3 1		1.604		4
4 4 0	–	1.529	–	1
4 0 2		1.521		2
5 2 1	–	1.504	–	< 1
5 3 0	–	1.483	–	1
3 3 2		1.476		< 1
6 0 0	1.43_4*	1.441	M	< 1
4 2 2		1.435		1
1 0 3	–	1.408	–	< 1
6 2 0	1.36_2	1.367	W	7
6 1 1	1.34_8	1.349	W	2
2 1 3		1.339		1
5 1 2		1.329		2
5 4 1	–	1.288	–	2
3 0 3		1.279		5
4 4 2	1.22_8	1.244	W	2
6 3 1		1.234		10
3 2 3		1.227		14
5 5 0	1.21_8	1.223	M	5
7 1 0		1.223		9
5 3 2		1.219		35
6 4 0	1.19_5	1.199	W	< 1
6 0 2		1.196		5
7 0 1	1.18_0	1.187	W	6
4 1 3		1.180		8

*Coincides with α-Fe(B) reflections.

difference between the structures of Fe_3B formed under atmospheric pressure and high pressure.

Generally speaking, annealing for a longer time or at a higher temperature is required to induce changes in the structure of the amorphous alloy subjected to high pressure. Fig. 3 shows the T–T–T diagram at 50 kbar. A shift in the location of the line dividing the amorphous and crystalline regions is clearly seen compared with Fig. 1. Another notable feature of crystallization under high pressure is that it always starts with simultaneous precipitation of α-Fe(B) and Fe_3B from the amorphous matrix. Hence the transformation is characterized as one occurring in a single step, in contrast to crystallization under atmospheric pressure occurring in two steps.

Cedergren and Bäckstrom [18] showed by means of electrical resistance measurements that T_c of $Fe_{80}B_{20}$ is raised with the application of pressure at a rate of 1.5 K kbar^{-1}. This is consistent with the results of the present work.

3.3. Crystallization under a pressure of 100 kbar

When the pressure is increased to 100 kbar, the amorphous state becomes more stable and the onset of crystallization is detected after a much longer annealing time at a much higher temperature.

Fig. 4 shows X-ray diffraction patterns of the alloy annnealed (a) at 460° C for 1260 min, and (b) at 460° C for 3150 min. In (a) all of the observed diffraction lines can be indexed in terms of the tetragonal structure of Fe_3B, while in (b) the lines are from Fe_3B plus a coexisting α-Fe(B). These facts show that the crystallization at 100 kbar occurs again in two steps and the crystalline phase wich appears first is not α-Fe(B) but Fe_3B. Measurement of the X-ray diffraction pattern shown in Fig. 4b has given a further increased lattice constant of α-Fe(B) appearing at the later stage of the crystallization.

The preferential formation of Fe_3B under high pressure is discussed in the following section.

4. Discussion

4.1. Comparison of the pressure effects on $Fe_{83}B_{17}$ with those on $Pd_{80}Si_{20}$

Iwasaki and Masumoto [6] observed an overall retardation of crystallization in pressurized $Pd_{80}Si_{20}$ alloy and ascribed this to a suppression of atomic diffusion involved in the crystallization process of the amorphous alloy. The same is also shown to be the case with $Fe_{83}B_{17}$. That diffusion over distances much longer than the nearest neighbour distance plays a significant role in the crystallization seems to be a feature common to the amorphous alloys prepared by the splat-quenching technique. The application of pressure

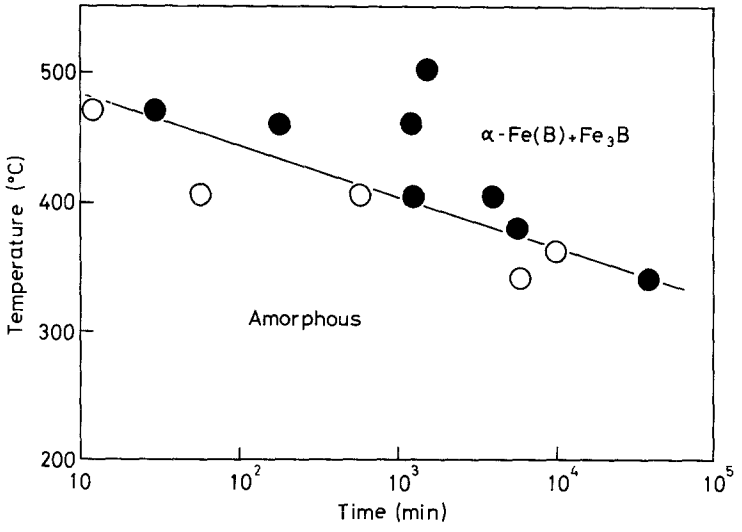

Figure 3 Time-temperature transformation diagram of amorphous $Fe_{83}B_{17}$ alloy on annealing at 50 kbar.

thus stabilizes the amorphous state and the alloys can retain a random arrangement of atoms up to higher temperatures. In $Pd_{80}Si_{20}$, formation of the MS-II phase, a metastable phase with a large unit cell, is suppressed under pressure and instead a metastable phase with only two atoms in the body centred tetragonal cell appears. No new phase is formed in pressurized $Fe_{83}B_{17}$ but the relative stability of the phases is changed. It can be said that the effect of pressure is more pronounced for $Pd_{80}Si_{20}$ than for $Fe_{83}B_{17}$.

4.2. Structural characteristics of Fe_3B and its preferential formation under pressure

During the past decades various attempts have been made to derive structure models for amorphous alloys and there are two models which seem to be attractive. In Polk's model [19] one assumes that metal atoms form a network of so-called dense-random-packing arrangements and metalloid atoms take interstitial positions in this network. The interstices most frequently found are those which are surrounded tetrahedrally and octahedrally by metal atoms, but their space is too small for metalloid atoms such as boron, carbon, silicon and phosphor to be accommodated. There exist other types of interstices which are surrounded by increased number of atoms and therefore have larger spaces. According to Polk those which can offer possible places for the metalloid atoms are the cavities of the three kinds of polyhedra with nine, ten and eight metals atoms respectively at their vertices, as shown in Fig. 5. Geometrical investigation of the network showed that the ratio of the number of these polyhedra to that of the metal atoms is about 2/10 which turns out to be the same as the maximum fraction of the metalloid atoms to be contained in the amorphous alloy and is in approximate agreement with the observed results. Gaskell [20] showed, from a slightly different point of view, that the

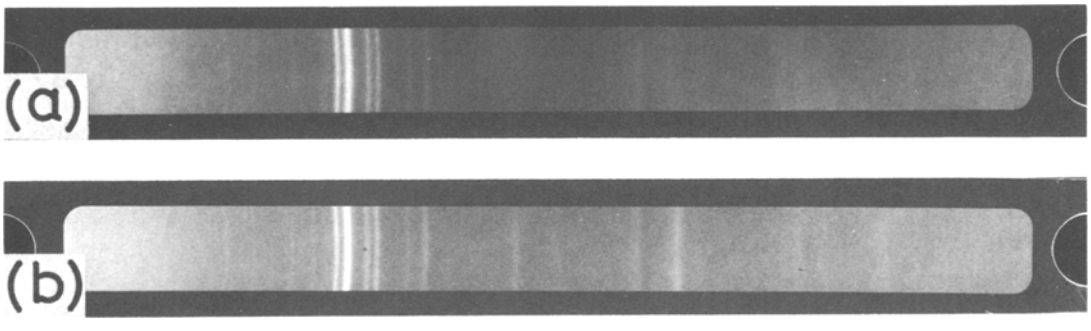

Figure 4 X-ray diffraction patterns of amorphous $Fe_{83}B_{17}$ alloy annealed (a) at 100 kbar and 460° C for 1260 min, and (b) at 100 kbar and 460° C for 3150 min.

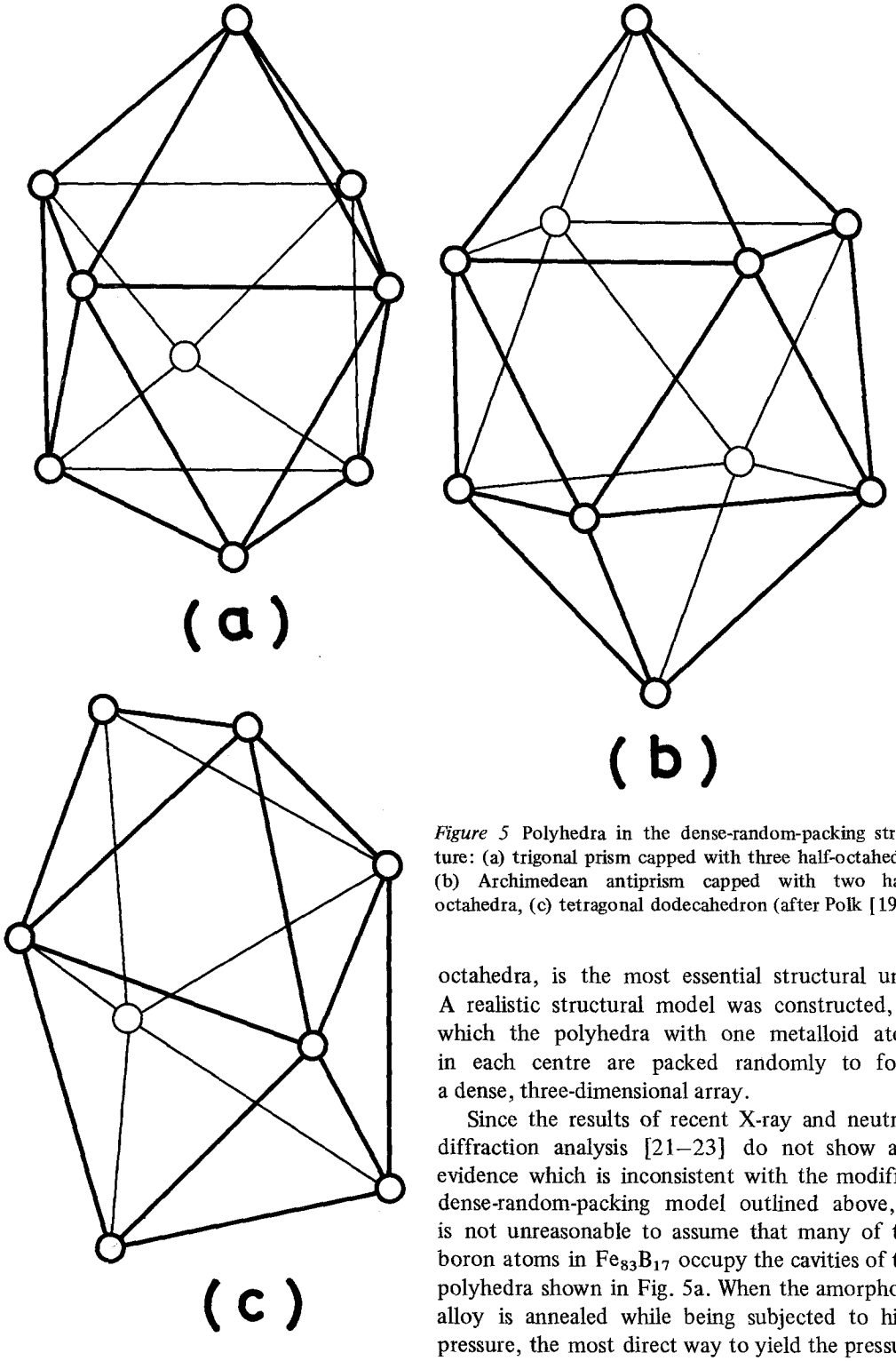

Figure 5 Polyhedra in the dense-random-packing structure: (a) trigonal prism capped with three half-octahedra, (b) Archimedean antiprism capped with two half-octahedra, (c) tetragonal dodecahedron (after Polk [19]).

local geometry around a metalloid atom in the amorphous alloy is very like that found in the crystalline metal borides, carbides, silicides and phosphides. The 9-atom polyhedron in Fig. 5a, which is a trigonal prism capped with three half-octahedra, is the most essential structural unit. A realistic structural model was constructed, in which the polyhedra with one metalloid atom in each centre are packed randomly to form a dense, three-dimensional array.

Since the results of recent X-ray and neutron diffraction analysis [21–23] do not show any evidence which is inconsistent with the modified dense-random-packing model outlined above, it is not unreasonable to assume that many of the boron atoms in $Fe_{83}B_{17}$ occupy the cavities of the polyhedra shown in Fig. 5a. When the amorphous alloy is annealed while being subjected to high pressure, the most direct way to yield the pressure is to change the atomic arrangement into a dense crystalline form with nearly identical local geometry and composition to those in the amorphous state. The structure of the metastable crystalline phase Fe_3B is of the Ni_3P type and schematically

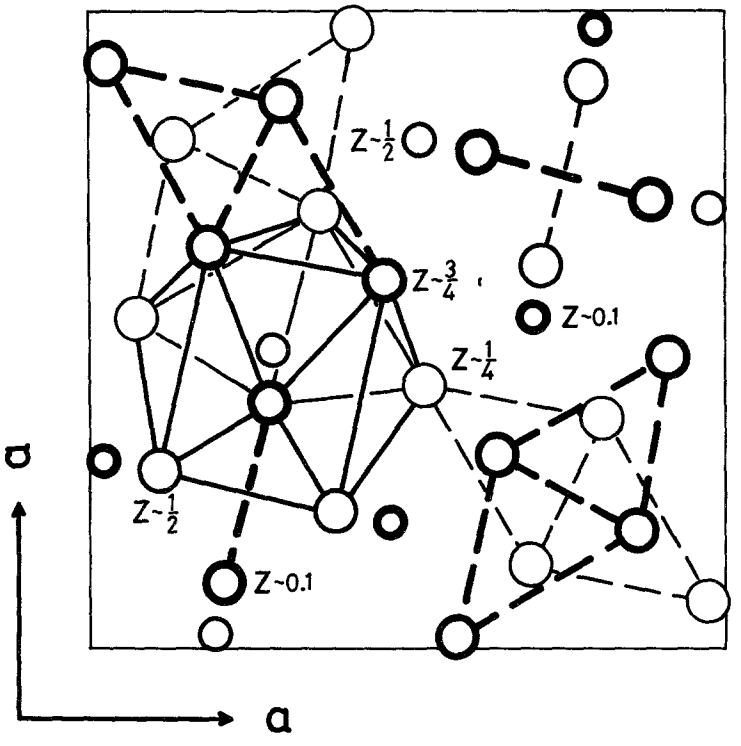

Figure 6 Atomic arrangement in Fe_3B. Large and small circles represent iron and boron atoms, respectively. Full lines mark one of the 9-atom-polyhedra containing a boron atom.

shown in Fig. 6. It is to be noted in this figure that every boron atom is located just at the centre of the 9-iron-atom polyhedron which we have seen in Fig. 5a. Full lines in Fig. 6 mark one of the polyhedra containing the boron atom. Transformation from the dense-random-packed structure to the Fe_3B structure is thought to be nucleated in the region where these polyhedra are neighbouring with each other and proceeds further with necessary rearrangement of iron and boron atoms around the nuclei. The origin of the preferential formation of Fe_3B under pressure is thus found to be similar to the local atomic arrangements of the amorphous structure.

4.3. Solid solubility of boron in iron

It is known that solid solubility of boron in α-Fe is extremely low. There has been controversy about which form, interstitially or substitutionally, boron atoms dissolve [24–26]. In previous structural studies on the crystallization of amorphous Fe–B, no accurate determination of the unit cell size of α-Fe precipitating from the amorphous matrix was made and nothing was made clear as to the solid solubility. As mentioned in Section 3, critical examination of X-ray diffraction patterns has shown that boron is dissolved as interstitial atoms in the iron lattice. From the observed concentration dependence of the lattice constant of Fe–C and Fe–N interstitial solid solution and the atomic size ratios of boron, carbon and nitrogen to that of iron, it is possible to estimate an approximate concentration of boron in α-Fe. This is 0.4 at% for the α-Fe formed at 100 kbar, large compared with the value 0.05 at% at 1 bar. Application of a much higher pressure will further suppress atomic diffusion and a solid solution richer in boron content will be obtained.

Acknowledgement

The authors wish to thank Prof. H. Kimura of the Research Institute for Iron, Steel and Other Metals for providing them with the high purity iron samples. They also wish to acknowledge helpful comments by Dr. T. Ichikawa.

References

1. T. MASUMOTO and R. MADDIN, *Mater. Sci. Eng.* **19** (1975) 1.
2. T. MASUMOTO, H. M. KIMURA, A. INOUE and Y. WASEDA, *ibid.* **23** (1976) 141.
3. T. MASUMOTO, Y. WASEDA, H. M. KIMURA and A. INOUE, *Sci. Rep. RITU* **A26** (1976) 21.
4. T. MASUMOTO, A. INOUE and H. M. KIMURA, *J. Japan Inst. Metlas* **41** (1977) 730.
5. W. C. EMMENS, J. VRIJEN and S. RADELAAR, *J. Non-Cryst. Solids* **18** (1975) 299.
6. H. IWASAKI and T. MASUMOTO, *J. Mater. Sci.*

13 (1978) 2171.
7. K. FUKAMICHI, M. KIKUCHI, S. ARAKAWA and T. MASUMOTO, *Solid State Commun.* **23** (1977) 955.
8. R. RAY, R. HASEGAWA, C. -P. CHOU and L. A. DAVIS, *Scripta Met.* **11** (1977) 973.
9. M. KIKUCHI, K. FUKAMICHI, T. MASUMOTO, T. JAGIELINSKI, K. I. ARAI and N. TSUYA, *Phys. Stat. Solid. (a)* **48** (1978) 175.
10. U. HEROLD and U. KÖSTER, *Z. Metallkde.* **69** (1978) 326.
11. J. L. WALTER, S. F. BARTRAM and R. R. RUSSELL, *Met. Trans.* **9A** (1978) 803.
12. T. KEMENY, I. VINCZE, B. FOGARASSY and S. ARAJS, *Phys. Rev.* **B20** (1979) 476.
13. H. S. CHEN and C. E. MILLER, *Rev. Sci. Instrum.* **41** (1970) 1237.
14. H. IWASAKI, Y. WATANABE and S. OGAWA, *J. Appl. Cryst.* **7** (1974) 611.
15. S. TAKAKI and H. KIMURA, *Scripta Met.* **10** (1976) 1095.
16. M. MATSUURA, *Solid State Commun.* **30** (1979) 231.
17. W. B. PEARSON, "A Handbook of Lattice Spacings and Structures of Metals and Alloys" Vol. 2 (Pergamon Press, Oxford, 1967) p. 248.
18. M. CEDERGREN and G. BÄCKSTROM, *J. Non-Cryst. Solid* **30** (1978) 69.
19. D. E. POLK, *Acta Met.* **20** (1972) 485.
20. P. H. GASKELL, *J. Non-Cryst. Solid* **32** (1979) 207.
21. Y. WASEDA and H. S. CHEN, *Phys. Stat. Sol. (a)* **49** (1978) 387.
22. T. FUKUNAGA, M. MISAWA, K. FUKAMICHI and T. MASUMOTO, Proceedings of the third International Conference on Rapidly Quenched Metals, Vol. 2, edited by B. Cantor (The Metals Society, London, 1978) p. 325.
23. N. COWLAM, M. SAKATA and H. A. DAVIES, *J. Phys. F* **9** (1979) L203.
24. W. R. THOMAS and G. M. LEAK, *Nature* **176** (1955) 29.
25. A. K. SHEVELEV, *Soviet Phys. Doklady* **3** (1958) 1254.
26. Y. HAYASHI and T. SUGENO, *J. Phys. Soc. Japan* **19** (1964) 1251.

Received 21 February and accepted 20 March 1980.